- Technical Paper -

STRESS-STRAIN MODELING OF CONFINED CONCRETE USING ARTIFICIAL NEURAL NETWORKS

Mingyang ZHANG[*1], Weilun WANG[*2], and Mitsuyoshi AKIYAMA[*3]

ABSTRACT

A stress-strain model was proposed based on the artificial neural networks (ANN) to predict the behavior of confined concrete columns under concentric compression. A wide range of previous experimental data including 182 samples were collected for establishing ANN model. Gauge length in the compressive test was used in the input layer of ANN model to take into consideration the difference of compressive fracture energy. The proposed stress-strain model provides good agreement with the test results independent of the compressive strength of concrete, yield strength of tie, and gauge length.

Keywords: confined concrete, compressive fracture energy, gauge length, artificial neural networks

1. INTRODUCTION

Confinement of core concrete is an important topic for the seismic design of reinforced concrete (RC) columns [1]. Numerous experimental studies on the behavior of confined concrete were conducted by many researchers [2-11]. Effect of concrete strength, and yield strength and spacing of transverse reinforcement on the stress-strain behavior has been examined based on the concentric loading test of RC columns. However, it is still difficult to estimate the stress-strain relation of RC columns accurately, independent of material strength, and structural details and dimensions. A computational method to take into consideration the effect of these parameters on the stress-strain relation of confined concrete has to be developed [12].

Artificial neural networks (ANN) is one of the optimal methods to describe the complex physical process and establish a nonlinear relationship between input and output parameters. Recently, the artificial neural networks have been widely used in the field of structural engineering. Oreta and Kawashima [13] proposed a neural network for predicting confined compressive strength and corresponding strain of circular concrete columns using 38 experimental data. Tang et al. [14] used the neural network techniques to predict the confinement efficiency of RC columns. The neural networks were trained with 45 samples and validated by comparing the computational and experimental results of the peak stress and the corresponding strain. Öztekin [12] developed an ANN model based on a large number and wide database with 252 experimental data for predicting the compressive strength of confined concrete. The developed ANN model predicted closer outputs to the experimental results than the analytical models with fewer errors. AL-Shatner [15] gathered experimental results for circular and square concrete columns to develop ANN for predicting the compressive strength of circular and square RC columns separately. For developing an ANN model which can completely model the complex interactions among the multiple variables, a sufficient number of data with a wide range is needed [13]. Although many ANN models were trained for estimating the strength and corresponding strain of confined concrete, studies on the full stress-strain modeling of RC columns considering post-peak behavior are scarce in the literature.

Localization occurs in compression failure of concrete [1, 16]. Stress-inelastic displacement can be used for calculating compressive fracture energy [17]. Akiyama et al. [1] pointed out that the stress-strain modeling of confined concrete based on the compressive fracture energy and the element length can give more accurate results, especially when the RC columns exhibit the post-peak behavior.

In this paper, a new model based on the ANN is proposed for predicting the behavior of confined concrete under concentric compression. The compressive fracture energy is adopted as a parameter in ANN model to establish the descending part of the stress-strain curve of confined concrete. A large amount of experimental data in the literature with wide ranges of each parameter are collected for training ANN. The stress-strain relation obtained by ANN are compared with the experimental results and the conventional model.

2. ARTIFICIAL NEURAL NETWORKS-BASED PREDICTION OF CONFINED CONCRETE

2.1 Description of ANN

Artificial neural network is a concept which was born due to the scientific interest about Artificial Intelligence (AI) during the middle of 1950 [18]. ANN are simplified models of a biological nervous system of the human brain. ANN models can be trained from the given information to establish a relationship between a set of input parameters and the output parameters. An ANN consists of two or more layers in which neurons

*1 Graduate School of Creative Science and Engineering, Waseda University, JCI Student Member
*2 Prof., Dept. of Civil Engineering, Shenzhen University
*3 Prof., Dept. of Civil and Environmental Engineering, Waseda University, JCI Member

are linked by weights. The summation of input data multiplied by the weights is modified by the activation function to get output data. The output data generated by neurons are either used as an input for next layer neurons or results for output layer (see Eq. 1).

$$Output = f\left(\sum_{i=1}^{n} a_i x_i + b\right) \quad (1)$$

where a_i is the *i-th* input data, b is the bias for the neuron, f is the activation function, and sigmoid function is preferred mostly as below:

$$f(x) = \frac{1}{1+e^{-x}} \quad (2)$$

The error between neural networks output and the desired value is calculated and back propagated to the networks to renew the weights and bias to decrease the error. Once the ANN is well trained, it can make prediction for output with any input set of data which is never appeared in the training set with an acceptable error. Most of the neural networks are based on the back-propagation algorithm. For the construction of ANN models, there is no reason to use any more than one hidden layer for the practical problem [19, 20].

2.2 Data collection

In this study, the data of total 182 samples were collected from the literature of RC columns under concentric compression conducted by eight teams [4-11]. The 182 datasets are divided into two separate datasets randomly, named training and testing datasets. 160 datasets are used for training the network and 22 datasets are used for validating the developed ANN model. The data contains a wide range of each parameter associated with the stress-strain relation. The shape and size of specimens for testing concrete strength are varied such as 150×300mm cylinder and cube. Therefore the concrete strength of each test is converted to that of 100×200mm cylinder strength using the empirical equations [21]. Peak stress and the corresponding strain of confined concrete, and strain at which stress drops to 50% of peak stress of confined concrete are available and easily obtained from the previous papers.

The compressive fracture energy $G_{f,c}$ is difficult to obtain because experimental full stress-strain curve of confined concrete is sometimes not available in the previous papers. It is assumed for obtaining $G_{f,c}$ from the literature that stress of confined concrete drops from the peak stress to 50% peak stress along a straight line from points *b* to *c* as shown in Fig. 1. The area of quadrangle *abcd* is equal to $G_{f,c}/L_m$.

$G_{f,c}$ can be expressed by

$$G_{f,c} = \frac{1}{2} f_{cc}\left[\frac{f_{cc}}{E_c} + \frac{3}{2}\left(\varepsilon_{c50} - \varepsilon_{cc}\right)\right] L_m \quad (3)$$

where f_{cc} (MPa) is the peak stress of confined concrete, ε_{cc} is the strain at peak stress of confined concrete, ε_{c50} is the strain corresponding to stress which drops to 50% peak stress, L_m (mm) is the gauge length, and E_c (in MPa) is the modulus of elasticity of unconfined concrete and is calculated by [22].

$$E_c = 3320\sqrt{f_{co}} + 6900 \quad (4)$$

where f_{co} (MPa) is unconfined concrete strength in member.

Therefore the experimental value $G_{f,c}$ was calculated by Eq. 3 based on the assumption shown in Fig. 1, and the experimental values (e.g., f_{cc}, ε_{cc}, etc.) from the past literatures. For establishing a neural network which can be used for predicting the behavior of both square and circular columns, effective confinement coefficient K_e is considered into the input layer in ANN, which is calculated by Eq. 5 for square cross-section, Eq. 6 for hoop and Eq. 7 for spiral reinforcement, respectively.

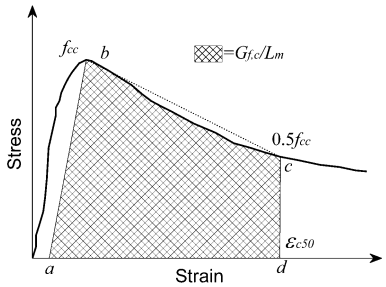

Fig. 1 Stress-strain relation with gauge length L_m

$$K_e = \frac{\left(1-\sum_{i=1}^{n}\frac{w_i^2}{6d_c^2}\right)\left(1-\frac{s'}{2d_c}\right)^2}{1-\rho_{cc}} \quad (5)$$

$$K_e = \frac{(1-\frac{s'}{2d_c})^2}{1-\rho_{cc}} \quad (6)$$

$$K_e = \frac{1-\frac{s'}{2d_c}}{1-\rho_{cc}} \quad (7)$$

where w_i (mm) is the *i*-th clear distance between adjacent longitudinal bars, s' (mm) is the clear spacing between transverse reinforcement, d_c (mm) is the core dimension of square and circular columns, and ρ_{cc} is the ratio of area of longitudinal reinforcement to area of core of section.

Fig. 2 shows the arcing action in confined concrete. The square and circular RC columns can be considered in one ANN models through K_e.

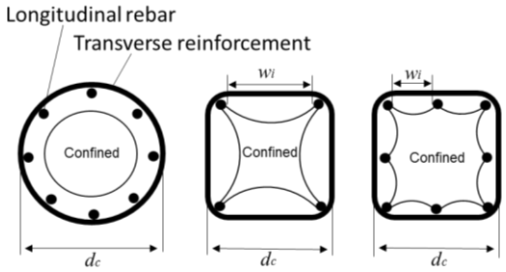

Fig. 2 Arcing action in confined concrete

2.3 Network Model

Total nine influencing parameters are considered

into the input layer of ANN-A, including core dimension of columns d_c (mm), height of specimen h (mm), gauge length L_m (mm), effective confinement coefficient K_e, the spacing of transversal reinforcement s (mm), area ratio of longitudinal steel ρ_{cc}, volumetric ratio of transversal steel ρ_s, strength of concrete f_c (MPa) and yield strength of transversal steel f_{yh} (MPa). For ANN-A pattern, the peak stress of confined concrete f_{cc} (MPa), strain at peak stress of confined concrete ε_{cc}, and compressive fracture energy $G_{f,c}$ (MPa·mm) were chosen as the output in the neural networks.

To examine the effect of gauge length on the accuracy of stress-strain relation, gauge length is not considered in the input layer in the ANN-B pattern. If the data of strain corresponding to 50% peak stress in descending part ε_{c50} is available in the literature, it is used directly as the third output neuron in the output layer in the ANN-B. The full stress-strain relation can be established based on ε_{c50} predicted by ANN model for describing the descending branch. The minimum and maximum values of each parameter are listed in Table 1.

Table 1 Structural details of RC column

Parameter	Minimum	Maximum
d_c (mm)	130	720
h (mm)	457	2400
L_m (mm)	203	1600
K_e	0.182	0.923
s (mm)	23	169
ρ_{cc}	0	0.05
ρ_s	0.0028	0.0727
f_c (MPa)	35	129
f_{yh} (MPa)	317	1387

For selecting the number of neurons in hidden layers, 10 models are developed with 11-20 neurons in hidden layers for each ANN patterns. The parameters used in ANN models are shown in Table 2. In this paper, a software, Multiple Back-Propagation (MBP) with back-propagation algorithm for training neural networks, was used for predicting the behavior of confined concrete.

Table 2 Input and output of ANN models

Layers	Input									Output			
Parameters	d_c	h	L_m	K_e	d	ρ_{cc}	ρ_s	f_c	f_{yh}	f_{cc}	ε_{cc}	ε_{c50}	$G_{f,c}$
ANN-A	√	√	√	√	√	√	√	√	√	√	√	×	√
ANN-B	√	√	×	√	√	√	√	√	√	√	√	√	×

Note: √ means the parameter is considered in ANN and × means the parameter is not used in ANN.

2.4 Model verification

The statistical parameters, OTR (*ANN output to desired target ratio*), MV (*mean value*), MAPE (*mean absolute percentage error*), SD (*standard deviation*) and COV (*coefficient of variation*) are used to verify the ANN model. These indices are expressed as following,

$$MV = \frac{1}{mn}\sum_{i=1}^{m}\sum_{j=1}^{n}\frac{O_{ij}}{T_{ij}} \tag{8}$$

$$SD = \sqrt{\frac{1}{mn}\sum_{i=1}^{m}\sum_{j=1}^{n}\left(1-\frac{O_{ij}}{T_{ij}}\right)^2} \tag{9}$$

$$MAPE = \frac{1}{mn}\sum_{i=1}^{m}\sum_{j=1}^{n}\left|\frac{T_{ij}-O_{ij}}{T_{ij}}\right| \tag{10}$$

where m, n, O, T are the number of output layer neurons, the number of test data, the output of a single neuron j and desire target for the single neuron j, respectively.

2.5 Model selection

For the two ANN patterns adopted in this paper, ANN-A and ANN-B with varying numbers of neurons from 11-20 in hidden layer were tested to choose the best model. Fig. 3 shows the statistical parameters SD and MAPE for each ANN models. The model selection is based on the results of SD and MAPE.

In ANN-A pattern, when the number of neuron in hidden layer is larger than 17, SD and MAPE increase slightly. When the number of hidden layer neurons is 20, SD and MAPE are equal to 0.563 and 0.248, respectively. As the number of neuron ranges from 11 to 16, SD and MAPE are variable and changing from 0.268 to 0.422 and from 0.192 to 0.253, respectively. When the number of neurons in hidden layer is 16, the optimum model is obtained with SD = 0.235 and MAPE = 0.158, respectively.

In ANN-B pattern, the SD starts from a larger value (i.e. 0.750), when the number of neurons in the hidden layer is 11. It decreases sharply to the minimum value (i.e. 0.376). The same trend is also confirmed in MAPE. Finally, 9-16-3 ANN model in pattern A and 8-12-3 ANN model in pattern B were chosen since both models can make a better prediction for the test results in each pattern. The two ANN structures are shown in Fig. 4.

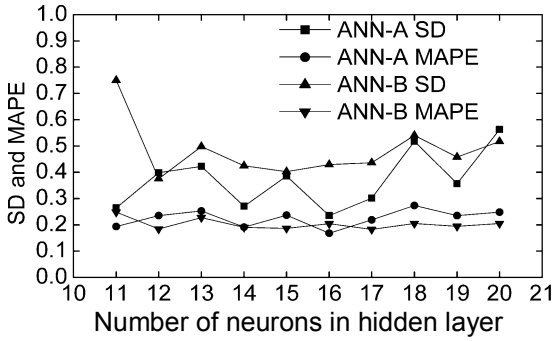

Fig. 3 Statistical results for two patterns

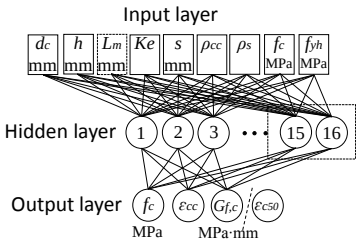

Fig. 4 ANN structure of two patterns

Table 3 ANN output to test result ratio

Sample	ANN-A 9-16-3			ANN-B 8-12-3		
	f_{cc}	ε_{cc}	$G_{f,c}$	f_{cc}	ε_{cc}	ε_{c50}
CC [9]	0.92	0.89	0.91	0.93	0.64	0.86
CG [9]	1.03	1.21	1.37	1.15	0.95	0.65
SI [9]	1.08	1.50	1.23	1.00	0.80	1.99
C [9]	0.98	0.97	1.05	0.98	1.00	0.74
fc40s50fy1288 [10]	0.95	0.97	1.29	1.01	0.92	1.26
fc80s25fy1288 [10]	1.04	1.01	0.64	1.03	0.80	0.59
fc80s100fy1288 [10]	0.90	0.98	1.52	0.95	0.70	0.97
fc120s100fy317 [10]	1.06	1.17	0.43	1.01	0.69	1.24
fc120s100fy1288 [10]	1.03	0.95	0.84	1.08	0.76	1.12
LH13LA [5]	0.96	1.32	0.83	1.02	1.63	1.34
HH13LB [5]	0.99	0.62	0.96	0.99	0.82	0.90
LL08LD [5]	1.04	1.68	0.60	1.02	1.30	0.56
1D [6]	0.97	1.12	1.29	1.03	0.75	1.42
3A [6]	1.01	0.65	0.64	0.83	0.89	0.89
5A [6]	1.01	1.18	0.78	1.04	0.68	1.21
8B [6]	0.96	0.84	1.16	0.95	0.87	1.10
Ca1m-1 [11]	1.14	0.95	1.41	1.08	0.95	1.14
Sa2s-1 [11]	1.02	0.98	0.41	1.05	0.66	0.42
Sb2s-2 [11]	1.00	1.08	1.18	0.99	0.78	0.89
Sb4l-2 [11]	0.92	0.86	0.86	0.91	1.11	0.80
H-D-25-S5.7-P53 [8]	0.86	1.24	1.00	0.95	0.73	0.80
VH-D20-S11.3P86 [8]	1.07	1.35	1.15	1.10	1.38	1.19
MEAN	1.00	1.07	0.98	1.00	0.90	1.00
COV	0.07	0.23	0.32	0.07	0.28	0.35

Table 3 lists the output results of two ANN models about the three prediction values f_{cc}, ε_{cc}, and $G_{f,c}$ (or ε_{c50}). They are ratio of computational to experimental values. It can be confirmed from these results that both ANN models can provide an accurate prediction of the f_{cc} value for each test sample.

For the $G_{f,c}$ and ε_{c50} predictions, it can be seen that the model in which L_m is considered in the input layer shows a slightly better result than that in which L_m is not considered in the input layer. COVs of $G_{f,c}$ and ε_{c50} in two ANN models are 0.323 and 0.348, respectively. While the error of MV is 0.022 for $G_{f,c}$ in pattern A which is larger than 0.003 in pattern B for ε_{c50}. The statistic results indicated that the ANN models can make accurate predictions for the values f_{cc}, ε_{cc}, and $G_{f,c}$ (or ε_{c50}) with lower errors. The results of COVs show the lower fluctuation of prediction of ANN models for experimental results. L_m is an important parameter in the compressive test for obtaining the strain in post-peak region. For the establishment of a stress-strain model of confined concrete, L_m has to be considered. In this study, the difference of results between two ANN models is not significant since the output of ANN model is not sensitive to the change in L_m.

3. MODEL FOR CONFINED CONCRETE

In previous literature, a number of models for confined concrete under concentric loading have been proposed computationally and experimentally. Table 4 shows an example of previous conventional models, which include f_{cc}, ε_{cc} and the mathematic expression for describing the stress-strain relationship of confined concrete. For establishing the relationship for confined concrete using the output of ANN models, the mathematical expressions of the ascending part originally proposed by Fafitis and Shah [2] was used herein. The mathematic expression of Fafitis and Shah model shows a good agreement with the ascending branch of experimental stress-strain curve of confined concrete. It has been widely used in many confined concrete models. It is expressed by Eq. 11. The descending part is determined assuming a straight line from the peak stress (point *b*) to the 50% of peak stress (point *c*) as shown in Fig. 1. The descending branch is expressed as Eqs. 12 and 13.

$$f_c = f_{cc}\left[1-\left(1-\frac{\varepsilon_c}{\varepsilon_{cc}}\right)^{\alpha}\right] \quad (0 \le \varepsilon_c \le \varepsilon_{cc}) \tag{11}$$

$$f_c = \frac{f_{cc}}{\varepsilon_{c50}-\varepsilon_{cc}}\left[\varepsilon_{c50}-0.5\left(\varepsilon_c+\varepsilon_{cc}\right)\right] \quad (\varepsilon_{cc} \le \varepsilon_c) \tag{12}$$

$$\varepsilon_{c50} = \varepsilon_{cc} + \frac{2}{3}\left(\frac{2G_{f,c}}{f_{cc}L_m} - \frac{f_{cc}}{E_c}\right) \tag{13}$$

$$\alpha = E_c\frac{\varepsilon_{cc}}{f_{cc}} \tag{14}$$

where f_c, f_{cc}, and E_c are in MPa, $G_{f,c}$ is in MPa·mm, and L_m is in mm.

The full experimental stress-strain curve of confined concrete was extracted from the literature. Previous nine experimental results were used for validating the stress-strain model. Fig. 5 shows the comparison of the results from the proposed model and experiment.

In all nine cases, the stress-strain relationship of confined concrete proposed in this paper based on the output of ANN model can accurately make the prediction for the experimental results. The results from Mander et al. [3] were only provided for normal strength concrete columns in Fig. 5. It is because the longitudinal strain in the experiment conducted by Mander et al. [3] was obtained over the central 450 mm (circular) and 400mm (square) gauge length of the columns, and their model was verified by the test results of the normal strength concrete columns. The proposed model can provide a good agreement with the experimental results independent of the concrete strength.

Table 4 Models for confined concrete

Refs.	Peak stress	Strain at peak stress	Model for confined concrete
[1]	$f_{cc}=f_{co}[2.28(p_e/f_{co})^{0.647}]$	$\varepsilon_{cc}=\varepsilon_{co}+0.0766(p_e/f_{co})$	$f_c=f_{cc}[1-(1-\varepsilon_c/\varepsilon_{cc})^{\alpha}]$ $f_c=f_{cc}\exp[k_d(\varepsilon_c-\varepsilon_{cc})^{k_d}]$
[3]	$f_{cc}=f_{co}(-1.254+2.254\sqrt{1+7.94f_l/f_{co}}-2f_l/f_{co})$	$\varepsilon_{cc}=\varepsilon_{co}[1+5(f_{cc}/f_{co}-1)]$	$f_c=f_{cc}xr/(r-1+x^r)$
[7]	$f_{cc}=f_{co}+k_1f_{le}$	$\varepsilon_{cc}=\varepsilon_{co}(1+5k_3k_1f_{le}/f_{co})$	$f_c=f_{cc}xr/(r-1+x^r)$

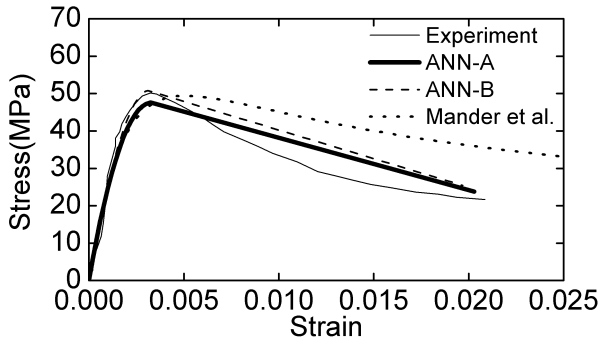

(a) fc40s50fy1288 [10]

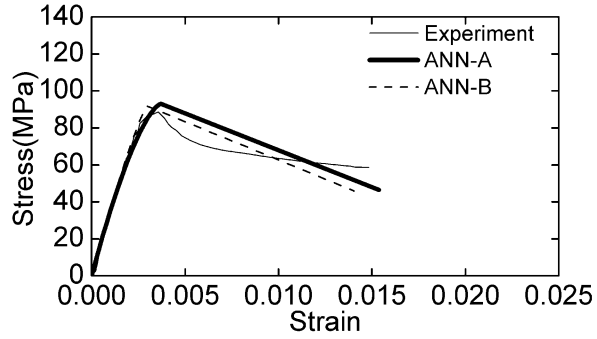

(b) fc80s25fy1288 [10]

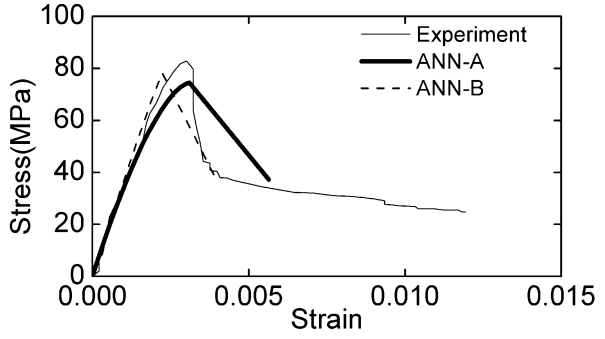

(c) fc80s100fy1288 [10]

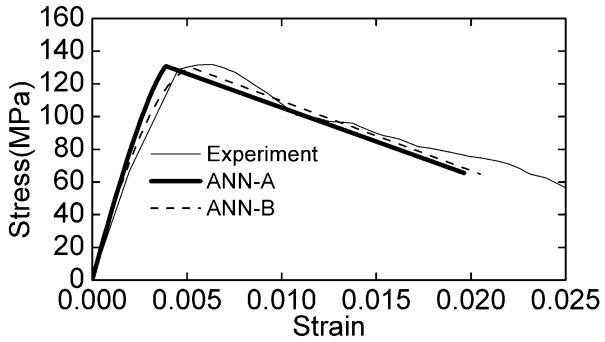

(d) HH13LB [5]

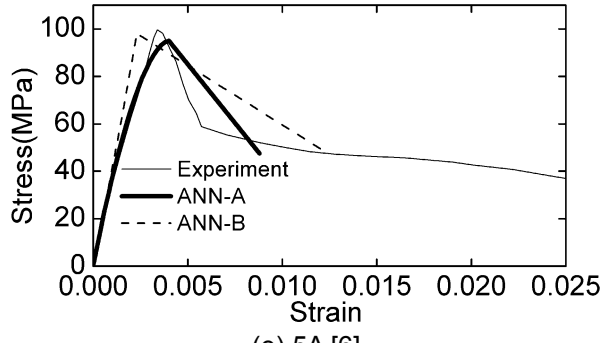

(e) 5A [6]

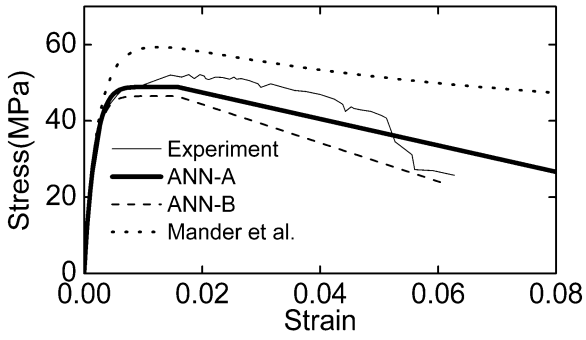

(f) Ca1m [11]

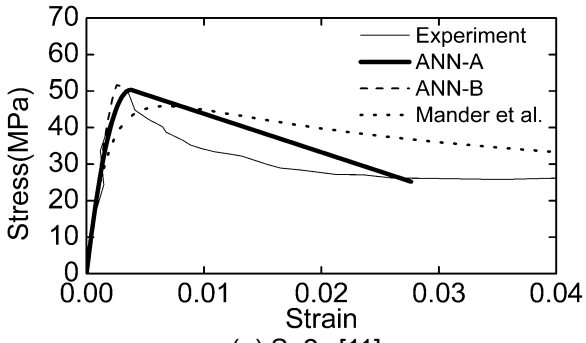

(g) Sa2s [11]

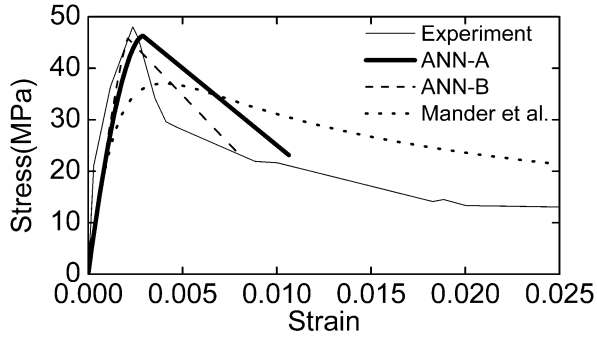

(h) Sb2s [11]

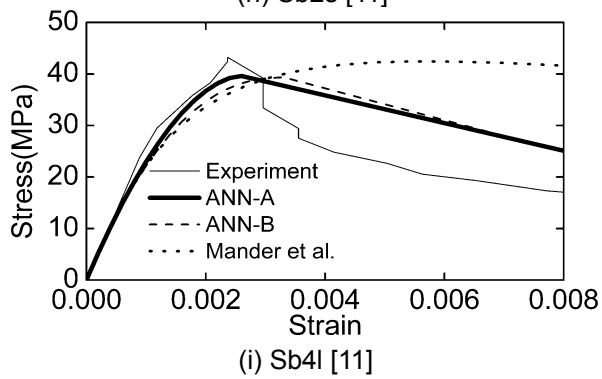

(i) Sb4l [11]

Fig. 5 Comparison of stress-strain relation from test results and from prediction by ANN and Mander et al. model [3]

4. CONCLUSIONS

The present study shows the feasibility of using artificial neural networks (ANN) model for predicting the behavior of confined concrete. Two kinds of ANN models for predicting the behavior of confined concrete under concentric compression were developed. Once the ANN model was trained, fixed mathematic network with weights and bias was obtained. Although this

mathematic network is an implicit model, it can be used easily to predict the behavior of confined concrete in practice.

(1) When the gauge length data in the experiment is used for training the network, the ANN model can give an accurate result of peak stress of confined concrete, strain at the peak stress and compressive fracture energy.

(2) The stress-strain relation for confined concrete established using two branch equations can provide good agreement with the test results compared with the conventional model.

(3) The proposed model gives reasonably good predictions for the experimental results, including the post-peak behavior of circular and square specimens with normal- to high-strength concrete (f_c=35-129 MPa) confined by normal- to high-strength reinforcement (f_{yh}=317-1387 MPa) of different volumetric ratios and arrangements.

ACKNOWLEDGEMENT

The experimental investigation about the behavior of confined concrete was supported by National Natural Science Foundation of China (Grant number: 51078236, 51378312) which is deeply acknowledged. The author also acknowledge the support of Shenzhen University, Shenzhen China.

REFERENCES

[1] Akiyama M., Suzuki M., Frangopol D. M., "Stress-averaged strain model for confined high-strength concrete," ACI Structural Journal, Vol. 107. 2010, pp. 179-188.

[2] Fafitis A., Shah S. P., "Lateral reinforcement for high-strength concrete columns," ACI Special Publication, Vol. 87. 1985, pp. 213-232.

[3] Mander J. B., Priestley M. J., Park R., "Theoretical stress-strain model for confined concrete," Journal of structural engineering, Vol. 114. 1988, pp. 1804-1826.

[4] Yong Y.-K., Nour M. G., Nawy E. G., "Behavior of laterally confined high-strength concrete under axial loads," Journal of Structural Engineering, Vol. 114. 1988, pp. 332-351.

[5] Nagashima T., Sugano S., Kimura H., Ichikawa A.,"Monotonic axial compression test on ultra-high-strength concrete tied columns," 10th World Conference on Earthquake Engineering, 1992, pp. 2983-2988.

[6] Cusson D., Paultre P., "High-strength concrete columns confined by rectangular ties," Journal of Structural Engineering, Vol. 120. 1994, pp. 783-804.

[7] Razvi S. R., "Confinement of normal and high-strength concrete columns," University of Ottawa 1995.

[8] Montgomery D. L., "Behavior of spirally reinforced high strength concrete columns under axial loading," University of Toronto, 1996.

[9] Sharma U. K., Bhargava P., "Behavior of confined high strength concrete columns under axial compression," Journal of Advanced Concrete Technology, Vol. 3. 2005, pp. 267-281.

[10] Hong K.-N., Han S.-H., Yi S.-T., "High-strength concrete columns confined by low-volumetric-ratio lateral ties," Engineering Structures, Vol. 28. 2006, pp. 1346-1353.

[11] Li Z.-b., Song J., Du X.-l., Yang X.-g., "Size effect of confined concrete subjected to axial compression," Journal of Central South University, Vol. 21. 2014, pp. 1217-1226.

[12] Öztekin E., "Prediction of confined compressive strength of square concrete columns by Artificial Neural Networks," International Journal of Engineering & Applied Sciences, Vol. 4. 2012, pp. 17-35.

[13] Oreta A. W. C., Kawashima K., "Neural network modeling of confined compressive strength and strain of circular concrete columns," Journal of Structural Engineering, Vol. 129. 2003, pp. 554-561.

[14] Tang C.-W., Chen H.-J., Yen T., "Modeling confinement efficiency of reinforced concrete columns with rectilinear transverse steel using artificial neural networks," Journal of Structural Engineering, Vol. 129. 2003, pp. 775-783.

[15] Al-Shather L. M., "Neural network prediction of confined peak stress of RC columns," Kufa journal of Engineering, Vol. 7. 2016, pp. 80-95.

[16] Cusson D., Larrard F. d., Boulay C., Paultre P., "Strain localization in confined high-strength concrete columns," Journal of Structural Engineering, Vol. 122. 1996, pp. 1055-1061.

[17] Nakamura H., Higai T., "Compressive fracture energy and fracture zone length of concrete," Modeling of inelastic behavior of RC structures under seismic loads, ASCE, 2001, pp. 471-487.

[18] Cascardi A., Micelli F., Aiello M. A., "An Artificial Neural Networks model for the prediction of the compressive strength of FRP-confined concrete circular columns," Engineering Structures, Vol. 140. 2017, pp. 199-208.

[19] Masters T., "Practical neural network recipes in C++," Morgan Kaufmann, 1993.

[20] Amani J., Moeini R., "Prediction of shear strength of reinforced concrete beams using adaptive neuro-fuzzy inference system and artificial neural network," Scientia Iranica, Vol. 19. 2012, pp. 242-248.

[21] Wille K., Naaman A. E., Parra-Montesinos G. J., "Ultra-High Performance Concrete with Compressive Strength Exceeding 150 MPa (22 ksi): A Simpler Way," ACI Materials Journal, Vol. 108. 2011, pp. 46-54.

[22] Carrasquillo R. L., Nilson A. H., Slate F. O.,"Properties of High Strength Concrete Subjected to Short Term Load," ACI Journal proceedings 1981, pp. 171-178.